Indian Journal of Pure & Applied Physics
Vol. 63, November 2025, pp. 1032-1043
DOI: 10.56042/ijpap.v63i11.22623

Influence of Sunspot Numbers and Solar Radio Flux on Geomagnetic Storm Activity during Solar Cycles 24 and 25

Swapnil Garg, Omkar Prasad Tripathi* & Saket Kumar
Department of Physics, AKS University, Satna 485 001, India

Received: 11th August 2025; accepted: 6th October 2025

This study systematically investigates the complicated link between solar activity indicators, specifically sunspot numbers (SSN) and solar radio flux (F10.7), and the occurrence of geomagnetic storms during Solar Cycles 24 and 25. The primary objective is to quantify the influence of these solar parameters on Earth's magnetospheric disturbances. The methodology involved a detailed analysis of 231 peak Disturbance Storm Time (Dst) events (P), 214 initial phase (P-I) geomagnetic storm events, and 201 recovery phase(P-R) geomagnetic storm events, all identified by a Dst threshold of ≤ -50 nT, covering the period from January 2008 to June 2024.

Statistical analysis, primarily through the calculation of Pearson correlation coefficients, revealed robust positive correlations. Peak Dst events exhibited correlation coefficients of 0.67 with sunspot numbers and 0.72 with solar radio flux. Similarly, geomagnetic storm events during the initial phase showed strong positive correlations with sunspot numbers (r = 0.69) and solar radio flux (r = 0.73). A comparable positive correlation was also observed during the recovery phase, with coefficients of 0.69 for sunspots and 0.73 for solar radio flux. A particularly striking finding was the exceptionally high correlation of 0.98 between the yearly average sunspot number and yearly average solar radio flux, underscoring the profound interconnectedness of these two solar parameters.

These findings highlight the significant predictive potential of sunspot numbers and solar radio flux in forecasting geomagnetic storm activity. The consistent strength of these correlations across different storm phases suggests that solar activity levels exert a sustained influence throughout the entire evolution of a geomagnetic disturbance, not merely its onset. Furthermore, the comparative analysis of Solar Cycle 24, which was historically weak, and the rapidly rising Solar Cycle 25 offers important clues about the evolving character of solar magnetic variability and its implications for space weather dynamics. The observed resurgence of activity in Cycle 25 implies a heightened likelihood of geo-effective space weather events compared to the preceding cycle.

Keywords: Disturbance storm time index (Dst), Solar activity, Sunspot number, Solar radio flux, Geomagnetic storm

1 Introduction

The Sun, our nearest star, is a dynamic and variable celestial body whose activity is inherently cyclical and governed by complex magnetic field dynamics originating within its interior and extending into interplanetary space[1,2]. This variability has a profound influence on the near-Earth space environment, a domain critical for modern technological infrastructure. Understanding and predicting these solar-terrestrial interactions, collectively known as space weather, is therefore of paramount importance[3-5].

1.1 Solar Activity and Its Manifestations

Solar activity manifests most prominently through two key indicators: sunspots and solar radio flux. Sunspots appear as dark, irregular patches on the Sun's photosphere, representing cooler regions where intense magnetic activity inhibits the convection of heat from the solar interior. These magnetically active regions often appear in groups and can persist for periods ranging from a few days to several months. Sunspot numbers have been systematically recorded for over two centuries, serving as a fundamental metric of solar activity and reflecting the underlying dynamo processes that generate and modulate the solar magnetic field[6,7].

Complementing sunspot counts is the Solar Radio Flux (F10.7), which quantifies solar radio emissions at a wavelength of 10.7 centimeters (or a frequency of 2800 MHz). This index is a crucial monitor of solar activity, closely associated with sunspot numbers, solar flares, and coronal mass ejections[8]. Unlike the subjective nature of visual sunspot counts, F10.7 flux provides a continuous, instrument-based measure of emissions originating from the upper chromosphere and lower corona. Its value is particularly significant

*Corresponding author: E-mail: omkar8415@gmail.com

because it correlates closely with solar ultraviolet (UV) and extreme ultraviolet (EUV) radiation, which are primary drivers of variability in Earth's ionosphere[9]. Both sunspot numbers and F10.7 are widely recognized as primary indicators of solar cycle progression and overall solar magnetic activity[10].

1.2 Geomagnetic Storms: Drivers and Impacts

Geomagnetic storms represent large-scale disturbances within Earth's magnetosphere, primarily initiated by enhanced coupling between the interplanetary magnetic field (IMF) and the terrestrial magnetic field. The principal drivers of these storms are coronal mass ejections (CMEs) and high-speed solar wind streams (HSS) emanating from coronal holes[3,11]. When these solar phenomena carry southward-directed magnetic fields and elevated plasma densities, they efficiently transfer substantial energy into Earth's magnetosphere through a process known as magnetic reconnection[4,7]. This energy injection leads to intensified geomagnetic currents, resulting in observable effects such as vibrant auroral displays, disruptions to radio communications (radio blackouts), anomalies in satellite operations, and the induction of geomagnetically induced currents (GICs) in terrestrial power grids. A notable historical example of such an impact is the March 1989 Hydro-Québec blackout, which underscored the severe vulnerabilities of critical infrastructure to intense space weather events[5,12].

1.3 The Significance of Solar Cycles 24 and 25

The period encompassing Solar Cycles 24 and 25, from 2008 to June 2024, offers a particularly compelling opportunity to study the solar-terrestrial connection. Solar Cycle 24 (2008-2019) was distinctive for its unusually low peak sunspot numbers and weak polar magnetic fields, marking it as one of the least active cycles in over a century[2, 6, 13]. This subdued solar activity was accompanied by a relatively low frequency of severe geomagnetic storms, prompting renewed interest in how various solar proxies relate to geo-effective events during weak cycles[7,11].

In stark contrast, Solar Cycle 25, which commenced in December 2019, has demonstrated a more rapid and robust rise in sunspot numbers and F10.7 flux. Preliminary observations indicate that several moderate to strong geomagnetic storms have already occurred early in Cycle 25, raising questions about whether a return to stronger solar and geomagnetic activity is underway[8,10].

The study of these relationships holds profound societal relevance due to the increasing reliance on modern technological infrastructure, which is highly susceptible to space weather disturbances. Robust predictive models of geomagnetic activity are essential for mitigating these risks, and such models depend on accurate, timely indicators of solar variability. Sunspot numbers and F10.7 radio flux remain among the most practical and reliable metrics for this purpose, owing to their long-term availability and strong empirical associations with eruptive solar phenomena[8,9,12].

Furthermore, investigating the variability of these indices over consecutive cycles provides an invaluable opportunity to understand how underlying solar dynamo processes manifest differently from cycle to cycle. The weak amplitude of Cycle 24, coupled with the relatively prolonged solar minimum preceding Cycle 25, had led to speculation regarding a broader trend toward declining solar activity. This hypothesis, if confirmed, would carry significant scientific and societal implications, given the potential impacts on the near-Earth space environment, climate variability, and operational planning for critical infrastructure. However, the early evolution of Cycle 25, characterized by a rapid increase in sunspot numbers and F10.7 flux, suggests that such long-term projections must be approached with caution. This rapid resurgence provides empirical evidence that challenges the immediate applicability of a grand minimum scenario, at least for the current cycle's progression, and points to a more complex, perhaps recovering, and solar dynamo behavior[13,14]. This underscores the critical importance of empirical studies that compare solar indices and geomagnetic storm outcomes in real time.

Beyond long-term trends, short-term variations in sunspot numbers and radio flux also serve as crucial signals for heightened probabilities of geo-effective events. For instance, sudden increases in F10.7 flux often accompany the emergence of large active regions on the Sun, which are more prone to producing powerful CMEs and flares capable of triggering significant geomagnetic storms[12]. Understanding the timing and magnitude of such variations relative to geomagnetic indices like Dst and Kp provides valuable insights into the intricate Sun-Earth coupling mechanisms[4,15].

1.4 Research Objectives

This study aims to systematically analyze the influence of sunspot numbers and solar radio flux on

the occurrence, frequency, and intensity of geomagnetic storms during Solar Cycles 24 and 25. By correlating monthly and annual trends in these solar activity indicators with documented geomagnetic disturbances, this research seeks to clarify how effectively these proxies can be used to anticipate space weather impacts under varying solar cycle conditions. The results are expected to inform operational forecasting, contribute to the broader understanding of solar-terrestrial interactions, and offer a comparative perspective on the evolving character of solar magnetic variability in the early 21st century.

2 Methodology

This section details the data sources, parameters, and statistical methods employed to investigate the relationship between solar activity and geomagnetic storm occurrences.

2.1 Data Sources and Period

The investigation encompassed two complete solar cycles, Solar Cycle 24 and the ascending phase of Solar Cycle 25, covering a comprehensive period from January 2008 to June 2024. All data utilized in this study were meticulously collected from the Omni Web Data Explorer, a widely recognized and reliable repository for solar-terrestrial data.

2.2 Solar Activity Parameters

Two primary solar activity parameters were examined in addition to their individual significance, sunspot number and F10.7 flux, which complement each other by capturing activity from different layers of the solar atmosphere, the photosphere and lower corona, respectively. Together, they provide a more comprehensive picture of solar magnetic variability. Their long-term continuity, strong correlation, and widespread availability make them ideal proxies for assessing the solar conditions that influence geomagnetic storm activity:

2.2.1 Sunspot Number (SSN)

Thisfundamental metric quantifies solar activity by counting the visible sunspots on the Sun's surface. It serves as a direct indicator of the magnetic activity on the photosphere[16].This fundamental statistic measures solar activity by measuring the number of visible sunspots on the Sun's surface[17]. It is a direct sign of magnetic activity on the photosphere, with sunspots appearing as darkening patches due to a high concentration of magnetic flux that locally restricts convective heat transmission. These zones are often thousands of kilometers in diameter and can arise alone or in complex clusters, changing on periods ranging from days to weeks[18].

Each sunspot has a high magnetic field, often reaching 1,000 gauss, that disrupts normal convection processes in the solar plasma. As a result, the afflicted region cools relative to its surroundings, making the sunspot appear darker. Because sunspot creation is inextricably linked to the solar magnetic cycle, monitoring their quantity gives a straightforward way to measure the strength and phase of the 11-year solar activity cycle. The Sunspot Number (also known as the International Sunspot Number) is calculated using a standardized formula that includes both individual sunspots and sunspot groups, with a correction factor to account for observational discrepancies. This makes it one of the most extensive and continuous databases in space research, with records dating back to the early 17th century. The Sunspot Number serves as a real-time indicator of current solar magnetic conditions and also acts as an important historical archive for studying long-term solar variability and its effects on Earth[15]. High sunspot counts are statistically linked to increased solar flares and coronal mass ejections (CMEs), making the Sunspot Number a crucial tool in both scientific research and practical space weather forecasting[19]. Analyzing its patterns helps improve models that predict disruptions in the Earth's magnetosphere and ionosphere. These disruptions can affect satellites, navigation systems, communication infrastructure, and even power grids on the ground.

2.2.2 Solar Radio Flux (F10.7)

Measured at a wavelength of 10.7 centimeters (2800 MHz), F10.7 provides a quantitative, instrument-based measure of solar emissions originating from the upper chromosphere and lower corona. It is a robust proxy for overall solar activity, closely correlated with other solar phenomena[16]. This radio flux index is one of the most consistent and dependable indicators of solar activity, collecting thermal bremsstrahlung (free-free) and gyro resonance emissions from active areas on the Sun. Unlike sunspot counts, which are dependent on eye observation and susceptible to observer bias and atmospheric conditions, the F10.7 indicator is based on continuous radiometric observations, providing consistency, impartiality, and worldwide comparability.

Since 1947, the F10.7 flux has been recorded daily from Ottawa, Canada, and later from Penticton. The flux is commonly reported in solar flux units (sfu),

with 1 sfu $=10^{-22}$ Wm^{-2} Hz^{-1}. Its long-term consistency and significant association with other solar indicessuch as sunspot number, EUV flux, and solar irradiancemake it especially useful for space weather study and simulation[18].

F10.7 is particularly significant because it represents not just observable surface activity (such as sunspots), but also high-energy events in the corona, which are vital for understanding ionospheric variability[20]. Short-term spikes in F10.7 flux frequently precede or coincide with the emergence of big sunspot groups, flares, and coronal mass ejections (CMEs)[21]. These fluctuations are important causes of changes in Earth's upper atmosphere, impacting thermosphere temperature, ionospheric density, and radio propagation tconditions[22].

Furthermore, because F10.7 flux significantly corresponds with solar ultraviolet (UV) and extreme ultraviolet (EUV) emissions, which are difficult to monitor constantly due to air absorption, F10.7 is an essential input for ionospheric and thermospheric models. It is commonly employed in satellite drag predictions, radio communication planning, and GNSS correction algorithms. To summarize, F10.7 is more than simply a numerical index; it is an important observational instrument that connects apparent solar activity to its radiative impacts on the near-Earth space environment, making it a necessary component of current heliophysics and operational space weather forecast systems[17].

2.3 Geomagnetic Storm Parameters

Geomagnetic storm activity was characterized using the Disturbance Storm Time (Dst) index, a globally recognized measure of the strength of the equatorial ring current, which is enhanced during geomagnetic storms. For this study, geomagnetic storm events were specifically identified by a threshold of Dst ≤ -50 nT, a criterion commonly used to classify moderate to strong storms.

The analysis categorized geomagnetic storm events into three distinct types:

2.3.1 Peak Dst Events (P):

A total of 231 geomagnetic storm events were analyzed, representing the maximum intensity reached by geomagnetic disturbances during the study period.

2.3.2 Geomagnetic Storm Events during Initial Phase (P-I):

This category included 214 geomagnetic storm events, which were less than the total number of peak geomagnetic events because some events had a difference between peak time and onset time that resulted in a threshold Dst of more than -50 nT, a value that corresponds to a sudden increase in the horizontal component of the geomagnetic field often associated with thearrival of a shock front or coronal mass ejection (CME) sheath at Earth.

2.3.3 Geomagnetic Storm Events during Recovery Phase (P-R):

A total of 201 geomagnetic storm events were analyzed which are less than the geomagnetic storm events for this phase because some events, difference between their peak time and recovery time resulted in a Dst threshold of more than -50 nT, which signifies the gradual return of the Dst index to its pre-storm levels, driven primarily by the decay of the ring current.

The classification of geomagnetic storm events into peak (P), initial phase (P-I), and recovery phase (P-R) can be understood in terms of the time lag between onset, peak, and recovery. Peak events (P) correspond to the moment when the Dst index reaches its lowest value, reflecting the maximum intensity of the storm. This peak always occurs after a certain lag from the onset as solar wind energy input strengthens the ring current. Initial phase events (P-I) are tied to the short lag between onset and peak. In some storms, the intensity of the Dst index drops rapidly below the threshold during this lag, while in others the intensification occurs more gradually, delaying the crossing of the threshold. Recovery phase events (P-R), on the other hand, are governed by the longer lag between the peak and the gradual return of the Dst index toward pre-storm levels. This lag represents the slow decay of the ring current, though in some cases the recovery may happen too quickly for the threshold condition to hold. Thus, the three categories reflect how differences in the timing of onset, peak, and recovery create variations in how storms are registered in each phase.

The consistent application of the Dst ≤ -50 nT threshold across all storm phases ensures that the analyzed events represent significant disturbances, thereby enhancing the reliability of the correlation analysis. The slight variations in the number of events across these phases (e.g., more peak Dst events than P-R) are expected, reflecting the complex and sometimes incomplete morphology of geomagnetic storms, where a storm might reach its peak intensity below the threshold but its initial or recovery phases might not always be distinctly classified under the

Table 1 — Annual Solar and Geomagnetic Activity Data (2008-2024)

S. No.	Year	No. of occurrences of Geomagnetic Storm (P)	No. of Occurrences of Geomagnetic Storm (P-I)	No. of Occurrences of Geomagnetic Storm (P-R)	Sunspot Number	Solar Radio Flux
1	2008	4	3	1	4	69.0
2	2009	1	1	1	5	70.5
3	2010	8	7	8	25	80.0
4	2011	12	12	12	81	113.3
5	2012	23	23	22	85	120.0
6	2013	22	21	19	94	122.7
7	2014	13	12	12	113	145.9
8	2015	27	27	28	70	117.7
9	2016	20	16	15	40	88.7
10	2017	16	15	13	22	77.3
11	2018	7	7	3	7	69.9
12	2019	6	4	3	4	69.7
13	2020	3	2	3	3	73.7
14	2021	9	8	7	30	81.6
15	2022	18	16	16	83	125.0
16	2023	23	21	21	125	159.7
17	2024	19	19	17	155	191.6

same strict criteria, or vice versa, depending on the specific definitions used by the data source. This consistency in methodology strengthens the validity of the comparative correlations reported.

2.4 Statistical Analysis Methods

The primary statistical method employed was correlation analysis, specifically the Pearson correlation coefficient ρX,Y. This method was used to quantify the linear relationship between the solar activity indicators (SSN and F10.7) and the occurrences of the various geomagnetic storm events.

The formula for the Pearson correlation coefficient is given by:

$$\rho X,Y = \mathrm{Cov}(X,Y)/\sigma X\,\sigma Y = E[(X-\mu X)(Y-\mu Y)]/\sigma X \sigma Y$$

where:

i. ρXY = Population correlation coefficient between variables X and Y
ii. μX = Mean of variable X
iii. μY = Mean of variable Y
iv. σX = Standard deviation of X
v. σY = Standard deviation of Y
vi. E = Expected value operator
vii. Cov = Covariance

This statistical approach allowed for a quantitative assessment of the degree to which changes in solar activity correspond to changes in geomagnetic storm frequency and intensity. The annual data used for this analysis is summarized in Table 1, providing the quantitative foundation for the subsequent graphical and statistical analyses presented in the results.

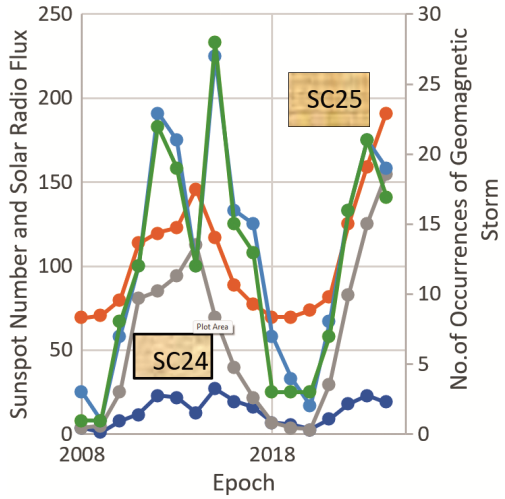

Fig. 1 — Represents the temporal evolution of solar and geomagnetic parameters from 2008 to 2024

3 Results

The analysis of solar activity indicators and geomagnetic storm occurrences across Solar Cycles 24 and 25 revealed clear temporal patterns and strong statistical correlations.

3.1 Temporal Evolution of Solar and Geomagnetic Parameters

The temporal evolution of sunspot numbers (SSN), solar radio flux (F10.7), and the frequencies of geomagnetic storm occurrences (P-I, P-R, and Peak Dst events) from 2008 to 2024 are comprehensively illustrated in Figs. 1-9. These figures collectively encompass the declining phase of Solar Cycle 23, the entirety of Solar Cycle 24, and the rapidly ascending phase of Solar Cycle 25.

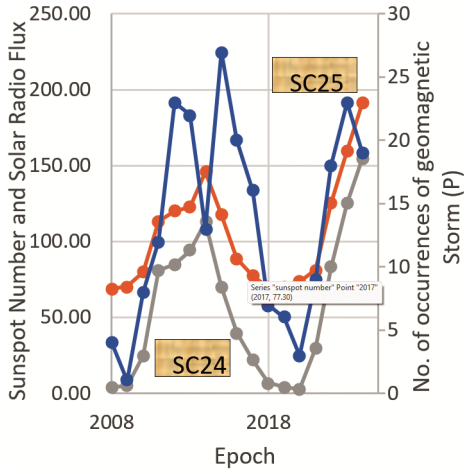

Fig. 2 — The figure illustrates the variation in sunspot numbers, solar radio flux, and the frequency of geomagnetic storm occurrences from 2008 to 2024

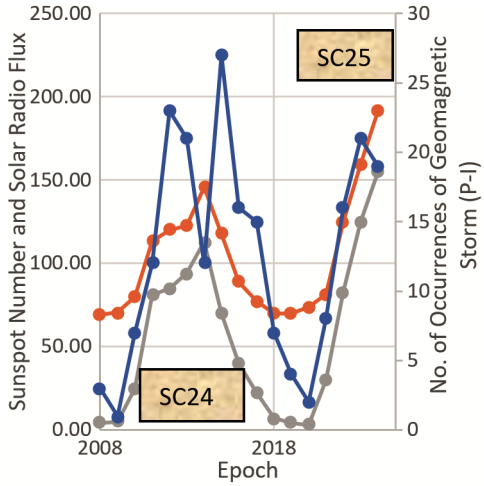

Fig. 3 — The figure illustrates the temporal evolution of three key parameters over the period spanning approximately 2008 to 2024

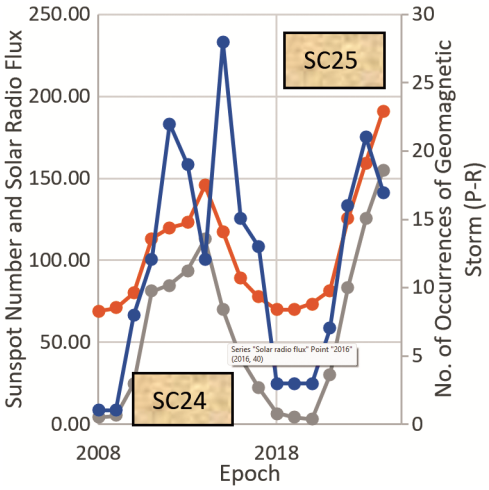

Fig. 4 — Figure illustrates the temporal variation of three principal indicators over the period from 2008 to 2024

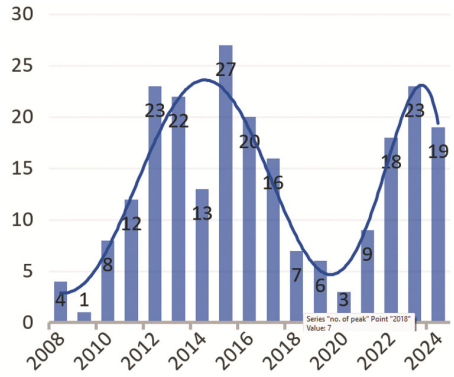

Fig. 5 — The hourly average no. of occurrences of geomagnetic storms

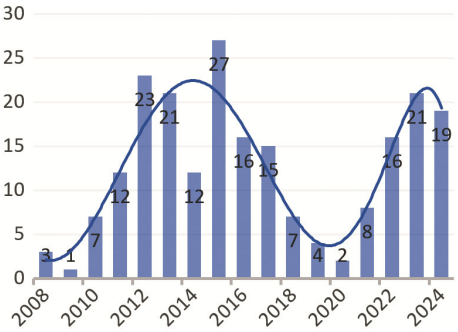

Fig. 6 — The hourly average no. of occurrences of geomagnetic storm (P-I)

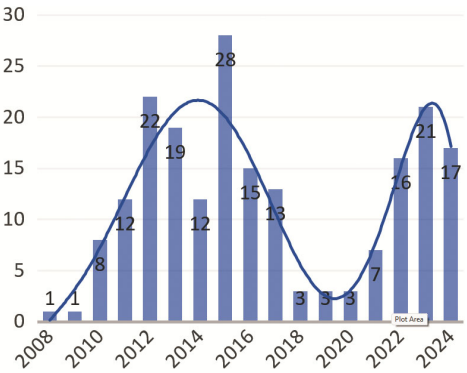

Fig. 7 — The hourly average no. of occurrences of geomagnetic storm (P-R)

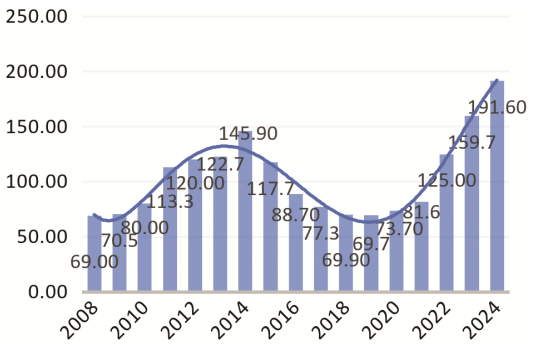

Fig. 8 — The yearly average solar radio flux

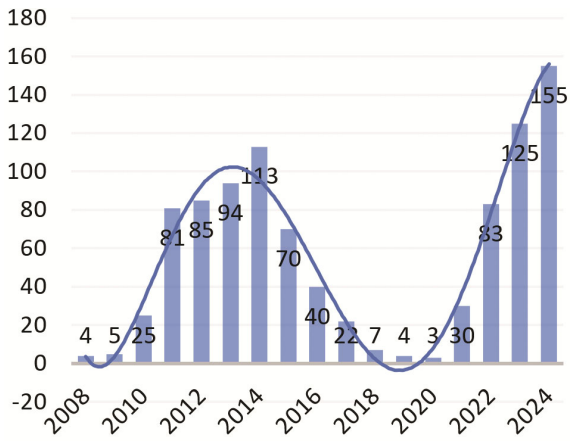

Fig. 9 — The yearly average sunspot number

Figures 1-4 present a holistic view of the synchronous evolution of solar and geomagnetic parameters. Sunspot numbers (orange curve/line) and solar radio flux (gray curve/line) consistently exhibit the characteristic approximately 11-year solar cycle. A pronounced increase in both parameters began around 2010, reaching a clear maximum between 2013 and 2015, which corresponds to the Solar Cycle 24 solar maximum. Specifically, in 2014, the sunspot number peaked at approximately 113, while the solar radio flux reached around 145.9 solar flux units (sfu). This peak was followed by a gradual decline toward the solar minimum observed near 2018-2019. A renewed and significant increase in both indicators is clearly evident after 2020, marking the robust rising phase of Solar Cycle 25. The synchronized progression of sunspot numbers and solar radio flux visually confirms their strong correlation as reliable indicators of solar magnetic activity.

As shown in Figs 1, 2, 3, and 4, the maxima in geomagnetic storm frequency broadly coincided with the peaks in solar activity. For instance, events with a difference between peak time and onset time (P-I) reached a peak of approximately 22 events during 2013-2015 and again rose to about 20 events in 2023-2024. Events with a difference between peak time and recovery time (P-R) demonstrated a similar temporal distribution, peaking near 15 events in 2014 and around 18 events in 2023, though occurring less frequently in absolute numbers. The total number of peak Dst events also followed this solar cycle modulation, reaching a maximum of about 25 peaks during 2014 and increasing again to 22 peaks by 2023.The number of occurrences of peak geomagnetic storm events varies in all three phases because when we find the difference between the peak time and the onset time, and the peak time and the recovery time,some of the events' threshold Dst is more than -50nT. Hence, peak geomagnetic storm events are 231;the difference between peak time and onset time of geomagnetic storm events is 214, and the difference between peak time and recovery time of geomagnetic storm events is 201.

Figures 5-7 further detail the annual occurrences of total geomagnetic storms, initial phase (P-I) events, and recovery phase (P-R) events, respectively. A prominent peak for all storm categories was observed around 2015 (28 events for total/P-R, 27 for P-I), followed by a gradual decline to a minimum around 2019-2020 (2-3 events), and then a secondary rise peaking in 2023 (21 events for P-I/P-R). The overlaid 6th-degree polynomial curves in these figures effectively illustrate these cyclical trends, reinforcing the approximately 11-year solar cycle's influence on geomagnetic activity.

Figures 8 and 9 specifically illustrate the annual variation of solar radio flux and sunspot numbers. Figure 8 shows solar radio flux values rising from approximately 69.0 SFU in 2008 to an initial peak of 145.9 SFU in 2014 (SC24 maximum), declining to a low near 69.9 SFU between 2018 and 2019 (solar minimum), and then rising sharply to a pronounced peak of 191.6 SFU by 2024. Similarly, Fig. 9 depicts sunspot numbers starting low in 2008-2009, peaking at 113 in 2014 (SC24 maximum), dropping to a minimum of 2-4 sunspots between 2018 and 2020, and then showing a strong resurgence to a projected peak of 155 by 2024 as SC25 progresses. These figures, with their overlaid 6th-order polynomial curves, clearly capture the wave-like progression characteristic of the 11-year solar cycle.

A particularly significant observation from these temporal analyses, especially evident in Fig. 2, is that by 2023-2024, sunspot numbers and geomagnetic storm occurrences were climbing rapidly, exceeding the previous cycle's peak levels. This strong resurgence in Solar Cycle 25, following the unusually weak Solar Cycle 24, has crucial implications for space weather forecasting and risk assessment. Given that SC24 was one of the least active cycles in over a century, the rapid and significant increase in both solar activity indicators and geomagnetic storm occurrences in SC25 suggests a return to more frequent and potentially more intense geo-effective events. This implies that critical infrastructure reliant

on space weather predictions, such as satellite operators, power grid managers, and communication networks, should anticipate a heightened risk environment compared to the previous cycle, necessitating updated risk mitigation strategies.

3.2 Correlation Analysis

The temporal analyses are further supported and quantified by scatter plots (Figs. 10-16) and the calculated correlation coefficients, which visually and

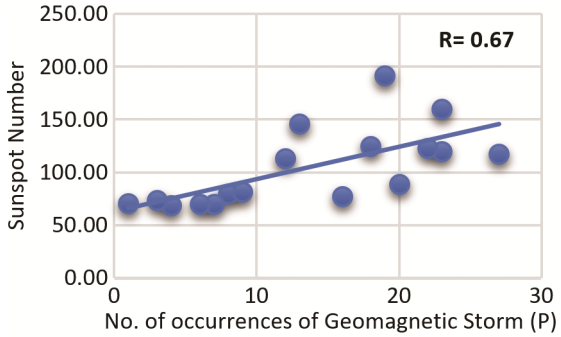

Fig. 10 — The scatter plot between No. of occurrences of geomagnetic storms and sunspot numbers

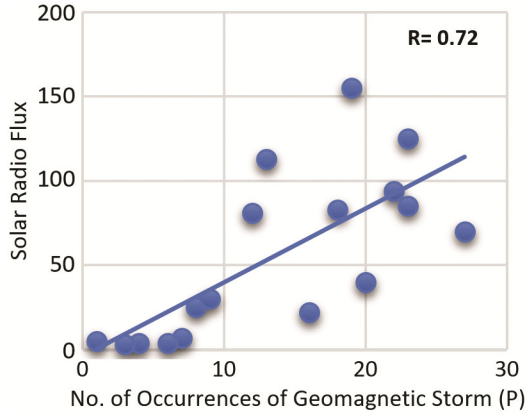

Fig. 11 — The scatter plot between No. of occurrences of geomagnetic storms and solar radio flux

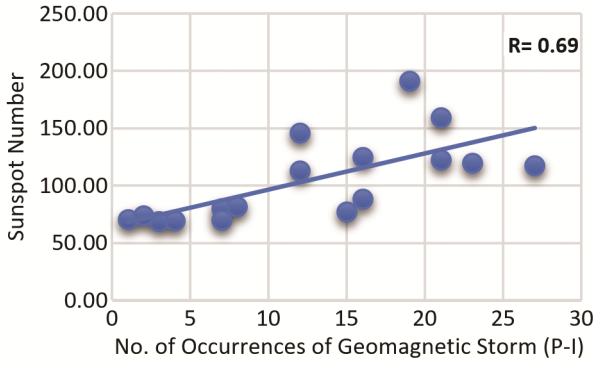

Fig. 12 — The scatter plot between No. of occurrences of geomagnetic storm (P-I) and sunspot number

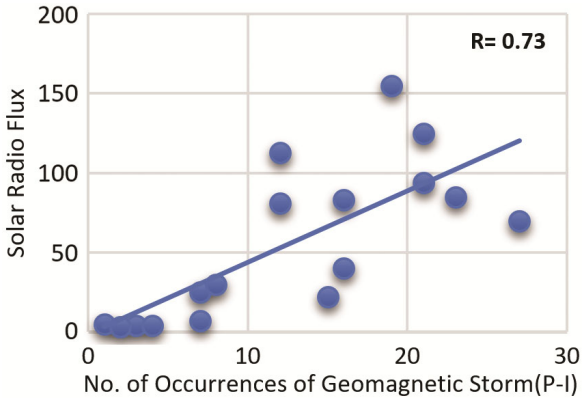

Fig. 13 — The scatter plot between No. of occurrences of geomagnetic storm (P-I) and solar radio flux

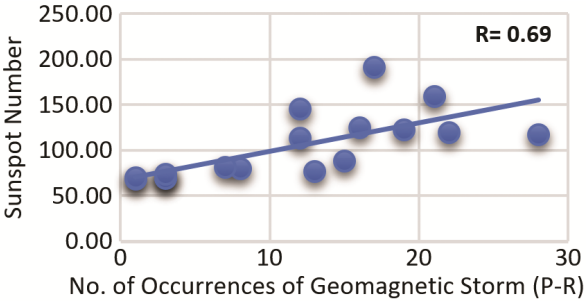

Fig. 14 — The scatter plot between No. of occurrences of geomagnetic storm (P-R) and sunspot number

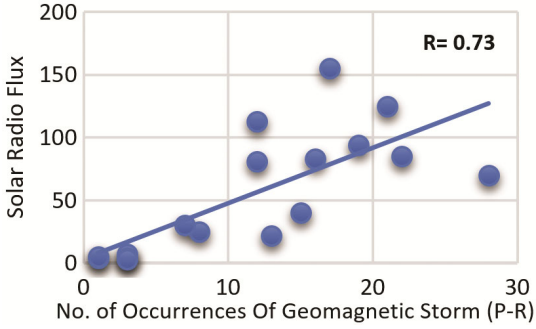

Fig. 15 — The scatter plot between No. of occurrences of geomagnetic storm (P-R) and solar radio flux

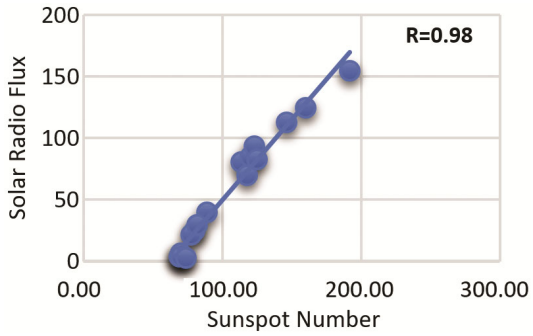

Fig. 16 — The scatter plot between sunspot number and solar radio flux

statistically demonstrate the relationships between solar activity and geomagnetic storm parameters.

The scatter plots generally illustrate positive relationships. For instance, Fig. 10 shows a visual trend of increasing geomagnetic storm occurrences with higher sunspot numbers, while Fig. 11 indicates that higher solar radio flux values correspond to more geomagnetic storm events. These visual trends are quantitatively confirmed by the correlation coefficients.

3.3 Geomagnetic Storm (Total/Peak Dst) vs. Solar Activity:

The total number of peak Dst events shows a positive correlation with sunspot numbers (r = 0.67).A slightly stronger positive correlation is observed between peak Dst events and solar radio flux (r = 0.72).

3.4 Initial Phase (P-I) Geomagnetic Storms vs. Solar Activity:

Figure 12 visually demonstrates a positive relationship between P-I events and sunspot numbers, with a correlation coefficient of 0.69.Figure 13 shows a strong positive relationship between P-I events and solar radio flux, with a correlation coefficient of 0.73.

3.5 Recovery Phase (P-R) Geomagnetic Storms vs. Solar Activity:

Figure 14 illustrates a positive trend between P-R events and sunspot numbers, with a correlation coefficient of 0.69.Figure 15 indicates a strong positive trend between P-R events and solar radio flux, with a correlation coefficient of 0.73.

Across all three geomagnetic storm, metrics (peak Dst, P-I, P-R), solar radio flux consistently exhibits a slightly higher correlation coefficient than sunspot numbers. While the difference is small, its consistency suggests that F10.7, being an instrument-based measure of solar emissions from the upper chromosphere and lower corona, might capture aspects of geo-effective solar activity (such as those related to CMEs and flares, which originate in these regions) more directly or sensitively than sunspot numbers, which are visual indicators of magnetic activity on the photosphere. This subtle distinction reinforces the value of F10.7 in operational space weather forecasting.

3.6 Sunspot Number vs. Solar Radio Flux:

Figure 16, a scatter plot of sunspot number against solar radio flux, visually demonstrates an exceptionally tight positive correlation, with data points clustering closely around a linear trend.

This visual observation is quantitatively supported by an exceptionally high correlation coefficient of 0.98 between yearly average sunspot number and yearly average solar radio flux. This exceptionally high correlation validates the use of these two distinct solar parameters as largely interchangeable proxies for the overall level of solar magnetic activity. While sunspot numbers provide a historical record spanning centuries and F10.7 offers continuous, objective measurements, their strong empirical link implies that long historical records of SSN can be reliably used to infer past F10.7 levels, and vice versa, enhancing the temporal depth and consistency of solar activity studies. However, as noted earlier, the slight difference in their individual correlation with geomagnetic storms (F10.7 marginally better) indicates that while highly correlated, they are not perfectly redundant. F10.7 might offer a subtle advantage for direct geo-effectiveness prediction due to its origin in the upper solar atmosphere, where geo-effective phenomena like CMEs and flares originate. This implies that while both are valuable, F10.7 could be prioritized for real-time operational forecasting, while SSN remains invaluable for historical context and cross-validation, especially for understanding long-term solar cycle behavior. A multi-proxy approach, leveraging the unique strengths of both indices, could lead to more robust and accurate space weather predictions, providing a more comprehensive picture of the solar-terrestrial environment.

4 Discussion

The findings of this study provide compelling evidence for the significant influence of solar activity on geomagnetic storm occurrences, particularly during Solar Cycles 24 and 25. The observed relationships offer critical insights into solar-terrestrial coupling and its implications for space weather forecasting.

4.1 Interpretation of Correlations and Temporal Trends

The analysis consistently revealed strong positive correlations between solar activity indicators (sunspot numbers and solar radio flux) and the frequency of geomagnetic storm occurrences, encompassing peak Dst, initial phase (P-I), and recovery phase (P-R) events. These statistical findings are visually reinforced by the consistent temporal alignment of peaks in solar activity and geomagnetic storm frequency across Figs 1-9. This alignment underscores the inherent cyclical nature of solar-terrestrial

coupling, with the polynomial fits in the figures further highlighting these underlying periodicities.

This alignment aligns with the well-established understanding that periods of elevated solar activity, particularly solar maxima, are characterized by a higher frequency and intensity of eruptive events, such as coronal mass ejections (CMEs) and solar flares. These phenomena are the primary drivers that inject energy and magnetic flux into Earth's magnetosphere, leading to the observed geomagnetic disturbances.

The consistent positive correlations across all three phases of geomagnetic storms (peak Dst, initial phase, and recovery phase) are particularly noteworthy. This suggests that the overall level of solar activity, as measured by sunspot numbers and F10.7, influences not just the probability of a storm occurring, but also its entire morphology and duration. Higher solar activity levels are likely to produce more energetic CMEs or more persistent high-speed streams. These drivers can induce stronger initial phases due to enhanced shock fronts and potentially longer-lasting recovery phases due to sustained energy injection into the ring current or more complex magnetospheric responses. This finding suggests a more comprehensive influence of solar activity on the entire storm process, underscoring the importance of these proxies for understanding the full lifecycle of geomagnetic disturbances.

4.2 Comparative Analysis of Solar Cycles 24 and 25

The study's comparative analysis of Solar Cycles 24 and 25 offers crucial insights into the evolving character of solar activity. Solar Cycle 24 (2008–2019) was indeed historically weak, characterized by unusually low peak sunspot numbers, weak polar magnetic fields, and a correspondingly low frequency of severe geomagnetic storms, making it one of the least active cycles in over a century.

In stark contrast, the early phase of Solar Cycle 25 (from December 2019 onwards) has demonstrated a rapid and robust escalation of both sunspot numbers and solar radio flux. This resurgence is a key finding of this research. The introduction noted speculation about a "broader trend toward declining solar activity" following the weak SC24 and prolonged solar minimum, a hypothesis with significant implications for long-term climate variability. However, the empirical observations from this study clearly show SC25's rapid rise, with sunspot numbers and F10.7 values by 2024 potentially exceeding SC24's peak. This real-time data from the early phase of SC25 provides crucial evidence that challenges the immediate applicability of the "grand minimum" hypothesis. While long-term trends cannot be definitively dismissed based on the analysis of just two cycles, the early strength of SC25 suggests that the solar dynamo might be recovering or exhibiting more complex variability than a simple linear decline. This has profound implications for long-term climate modeling, as solar activity is a known natural forcing factor, and refutes the notion of an immediate, sustained reduction in solar irradiance and associated terrestrial impacts.

The observed strength of Solar Cycle 25 implies a higher likelihood of geo-effective space weather events compared to Solar Cycle 24. This shift in activity levels necessitates updated preparedness and mitigation strategies for space weather impacts on critical technological infrastructure.

4.3 Predictive Value for Space Weather Forecasting

This research strongly reinforces the predictive value of sunspot numbers and the F10.7 index as practical and reliable proxies for anticipating geomagnetic storm risk. These indices provide timely indicators for operational forecasting, which is crucial for mitigating the impacts on modern technological infrastructure, including satellites, electrical power grids, and communication systems. The historical example of the March 1989 Hydro-Québec blackout serves as a stark reminder of such vulnerabilities.

The study confirms the strong correlation of both sunspot numbers and F10.7 with geomagnetic storms, but F10.7 consistently shows slightly higher correlation coefficients (0.72-0.73 vs. 0.67-0.69). While sunspot numbers benefit from a longer historical record, providing valuable context for long-term trends, F10.7 offers continuous, instrument-based measurements, which are inherently less subjective. This suggests that for real-time operational forecasting, F10.7 might be the preferred primary proxy due to its slightly better correlation and objective measurement. However, sunspot numbers remain invaluable for historical context and cross-validation, especially for understanding long-term solar cycle behavior. A multi-proxy approach, leveraging the unique strengths of both indices, could lead to more robust and accurate space weather predictions, providing a more comprehensive picture of the solar-terrestrial environment. This dual role underscores their utility for both long-term (solar

cycle progression, general activity levels) and short-term (imminent storm potential) forecasting.

4.4 Limitations and Future Work

While this study provides significant contributions, it is important to acknowledge certain limitations. The reliance on annual averages, while useful for identifying cyclical trends, may smooth out the nuances of short-term, intense events. The specific Dst threshold of -50 nT, while standard for moderate to strong storms, excludes weaker geomagnetic disturbances. Furthermore, the focus on only two solar cycles, albeit critical ones, limits the ability to identify more generalized patterns or deviations across a broader historical context.

Future research should build upon these findings by:

i Extending the analysis to a broader range of solar cycles to identify more generalized patterns or deviations in solar-terrestrial coupling.

ii Refining the understanding of how short-term fluctuations (e.g., daily or hourly) in sunspot numbers and F10.7 relate to specific storm intensities and durations, moving beyond annual correlations.

iii Investigating the influence of other solar wind and interplanetary magnetic field parameters (e.g., solar wind speed, IMF Bz, CME properties) in conjunction with sunspot numbers and F10.7 for more comprehensive and nuanced space weather prediction models.

iv Exploring the lead-lag relationships between solar proxies and geomagnetic storms more deeply, to establish precise predictive timings.

5 Conclusion

This study conclusively demonstrates that solar activity indicators, specifically sunspot numbers and solar radio flux, exert a measurable and statistically significant influence on geomagnetic storm occurrences during Solar Cycles 24 and the rising phase of Cycle 25. Time series analyses clearly illustrate that periods of elevated sunspot numbers and higher solar radio flux consistently coincide with increased frequencies of geomagnetic storms, reflected across the initial phase (P-I), recovery phase (P-R), and peak Dst events.

The observed correlation coefficients further substantiate this robust relationship. Sunspot numbers show strong positive correlations with geomagnetic storm activity, exhibiting coefficients of approximately 0.69 across the initial and recovery phases, and 0.67 with the number of peak occurrences. Solar radio flux exhibits similarly strong correlations with geomagnetic storm activity, with coefficients reaching approximately 0.73 across the initial and recovery phases, and 0.72 with the number of peak geomagnetic storm occurrences. Notably, an exceptionally high correlation of 0.98 was found between yearly average sunspot numbers and yearly average solar radio flux, underscoring their intrinsic connection as complementary measures of solar magnetic activity.

A crucial comparative insight from this research is the stark contrast between Solar Cycle 24, which was historically weak, and the rapid escalation of sunspot numbers and radio flux observed in Solar Cycle 25. This resurgence suggests a higher likelihood of geo-effective space weather events in the current cycle compared to the preceding one. This finding also provides empirical data that challenges immediate projections of a long-term decline in solar activity, suggesting a more complex behavior of the solar dynamo.

Overall, this research reinforces the predictive value of sunspot numbers and the F10.7 index as practical proxies for anticipating geomagnetic storm risk. As technological reliance on space-based systems continues to grow, the continued monitoring and integration of these indices into forecasting models will remain critical for mitigating the impacts of geomagnetic disturbances on infrastructure, communications, and power systems. This study contributes to the broader understanding of solar-terrestrial interactions and space weather dynamics, advocating for ongoing research and refined modeling to enhance preparedness for future space weather events.

References

1 Charbonneau P, *Living Rev Sol Phys,* 17 (1) (2020) 4.
2 Hathaway D H, *Living Rev Sol Phys*, 12 (1) (2015) 4.
3 Gopalswamy N, *Space Sci Rev*, 124 (1) (2006) 145.
4 Gonzalez W D, Joselyn J A, Kamide Y, Kroehl H W, Rostoker G, Tsurutani B T & Vasyliunas V M, *J Geophys Res*, 99 (4) (1994) 5771.
5 Boteler D H, *Space Weather*, 17 (10) (2019) 1427.
6 Clette F, Svalgaard L, Vaquero J M & Cliver E W, *Space Sci Rev*, 186 (1) (2014) 35.
7 Kumar S, Tripathi O P, Sharma R & Verma P L, *J Phys: Conf Series*, 2576 (1) (2023) 012015.
8 Tapping K F, *Space Weather*, 11 (7) (2013) 394.
9 Dudok de Wit T, Kretzschmar M, Lilensten, J & Woods T N, *Geophys Res Lett*, 36 (10) (2014) 1.
10 Kilcik A, Ozguc A, Rozelot J-P & Atac T, *Sol Phys*, 270 (1) (2011) 75.

11 Pulkkinen A, *Living Rev Sol Phys*, 4 (1) (2007) 1.
12 Kappenman J G, *Space Weather*, 3 (8) (2005).
13 Pesnell W D, Space Weather, 14 (1) (2016) 10.
14 Lean J L, *WIREs Climate Change*, 1 (1) (2010) 111.
15 Svalgaard L & Cliver E W, *J Geophys Res*, 112 (10) (2007) 1.
16 Clette F, *J Space Weather Space Climate*, 11 (2021) 2.
17 Mursula K, Asikainen T & Holappa L, *Astronomy & Astrophys*, 683 (2024) A 27.
18 Tripathi O P & Verma P L*, Ind J Appl Res*, 3 (5) (2013) 47.
19 Verma P L & Tripathi O P, *Int J Innovative Res Growth*, 2 (2016) 115.
20 Tripathi O P & Verma P L, *Ind J Sci Res*, 2 (2013) 7.
21 Gopalswamy N, Michalek G, Yashiro S, Makela P, Akiyama S & Xie H, *Astrophys J,* 952 (2023).
22 Dagnew F K, Gopalswamy N, Tessema S B, Akiyama S & Yashiro S, *Astrophys J,* 936 (2022) 122.